

How do the properties of a glass depend on the cooling rate? A computer simulation study of a LennardJones system

Katharina Vollmayr, Walter Kob, and Kurt Binder

Citation: *J. Chem. Phys.* **105**, 4714 (1996); doi: 10.1063/1.472326

View online: <http://dx.doi.org/10.1063/1.472326>

View Table of Contents: <http://jcp.aip.org/resource/1/JCPSA6/v105/i11>

Published by the [American Institute of Physics](#).

Related Articles

Structural phases in non-additive soft-disk mixtures: Glasses, substitutional order, and random tilings
J. Chem. Phys. **135**, 224515 (2011)

Topological origin of stretched exponential relaxation in glass
J. Chem. Phys. **135**, 214502 (2011)

Lumping analysis for the prediction of long-time dynamics: From monomolecular reaction systems to inherent structure dynamics of glassy materials
J. Chem. Phys. **135**, 204507 (2011)

Surface rippling on bulk metallic glass under nanosecond pulse laser ablation
Appl. Phys. Lett. **99**, 191902 (2011)

Construction of a disorder variable from Steinhardt order parameters in binary mixtures at high densities in three dimensions
J. Chem. Phys. **135**, 174109 (2011)

Additional information on *J. Chem. Phys.*

Journal Homepage: <http://jcp.aip.org/>

Journal Information: http://jcp.aip.org/about/about_the_journal

Top downloads: http://jcp.aip.org/features/most_downloaded

Information for Authors: <http://jcp.aip.org/authors>

ADVERTISEMENT

**AIP**Advances

Submit Now

Explore AIP's new
open-access journal

- Article-level metrics now available
- Join the conversation! Rate & comment on articles

How do the properties of a glass depend on the cooling rate? A computer simulation study of a Lennard-Jones system

Katharina Vollmayr,^{a)} Walter Kob,^{b)} and Kurt Binder

Institut für Physik, Johannes Gutenberg-Universität, Staudinger Weg 7, D-55099 Mainz, Germany

(Received 26 December 1995; accepted 12 June 1996)

Using molecular dynamics computer simulations we investigate how the glass transition and the properties of the resulting glass depend on the cooling rate with which the sample has been quenched. The system we study is a two component Lennard-Jones model which is coupled to a heat bath whose temperature is decreased from a high temperature, where the system is a liquid, to zero temperature, where the system is a glass. The temperature T_b of this heat bath is decreased linearly in time, i.e. $T_b = T_i - \gamma t$, where γ is the cooling rate, and we study the cooling rate dependence by varying γ over several orders of magnitude. In accordance with simple theoretical arguments and with experimental observations we find that the glass transition, as observed in the specific heat and the thermal expansion coefficient, becomes sharper when γ is decreased. A decrease of the cooling rate also leads to a decrease of the glass transition temperature T_g and we show that the dependence of T_g on γ can be rationalized by assuming that the temperature dependence of the relaxation times of the system is given by either a Vogel–Fulcher law or a power law. By investigating the structural properties of the glass, such as the radial distribution functions, the coordination numbers and the angles between three neighbor-sharing particles, we show how the local order of the glass increases with decreasing cooling rate. The enthalpy H and the density ρ of the glass decrease and increase, respectively, with decreasing γ . By investigating the γ dependence of clusters of nearest neighbors, we show how the cooling rate dependence of H and ρ can be understood from a microscopic point of view. Furthermore we demonstrate that the frequency of icosahedral-like structures is decreasing with decreasing cooling rate. We also show that the spectrum of the glass, as computed from the dynamical matrix, shows a shift towards higher frequencies when γ is decreased. All these effects show that there is a significant dependence of the properties of glasses on the cooling rate with which the glass is produced. © 1996 American Institute of Physics. [S0021-9606(96)50135-2]

I. INTRODUCTION

If a liquid is cooled rapidly enough, so that the crystallization at or slightly below the melting point is avoided, the final state of the material will be an amorphous solid, i.e. a glass. This so-called glass transition, i.e., the transition from a liquid state to an amorphous solid state, is essentially the falling out of equilibrium of the system, because the relaxation times of the system at the glass transition temperature exceed the time scale of the experiment. Thus the resulting glass is not in thermal equilibrium and it can therefore be expected that the properties of the glass will in general depend on the production history of the glass, as, e.g., the cooling rate with which the sample was cooled or, if the glass transition is pressure driven, on the rate with which pressure was applied. That such dependencies exist indeed has been shown in various experiments in which it was investigated how the density of the glass, the glass transition temperature, the specific heat or the Mössbauer spectrum depend on the cooling rate.^{1,2}

The dependence of the properties of a structural glass on

its production history have also been studied in computer simulations. Fox and Andersen have investigated for a one-component Lennard-Jones system the dependence of the density on the cooling rate³ and Baschnagel *et al.* have studied how various properties of a polymer glass depend on the cooling rate.⁴ However, because of their relatively complex model, the authors of this last work were able to vary the cooling rate by only two decades. Lai and Lin investigated the dependence of the Wendt–Abraham parameter on the cooling rate⁵ and Miyagawa and Hiwatari gave evidence that for their binary soft sphere model the structural properties of the glass are independent of the cooling rate, that, however, dynamical quantities depend on the cooling rate.⁶ Also Speedy investigated this type of question and reports that the rate with which a system of hard spheres is compressed does not affect the density of the glass.⁷

Thus although computer simulations are in principle a very useful tool in order to investigate the production history dependence of the properties of glasses, since they allow one to study a glass in its full microscopic details, relatively few simulations have been done to address this question in detail. One reason for this is that the effects to be expected are relatively small, usually on the order of a few percent when the cooling rate is varied by two or three decades,^{1,2} and that therefore the statistical accuracy of the data has to be rather high in order to detect these effects at all. However, as the

^{a)}Present address: Institute for Physical Science and Technology, University of Maryland, College Park, MD 20742.

Electronic mail: vollmayr@moses.physik.uni-mainz.de

^{b)}Author to whom all correspondence should be addressed.

Electronic mail: kob@moses.physik.uni-mainz.de http://www.cond-mat.physik.uni-mainz.de/~kob/home_kob.html

cited papers have shown, this problem is not insurmountable and the potential payoff of such types of computer simulations, namely to understand from a *microscopic* level how the production history of the glass affects its macroscopic properties, seems to justify the effort involved.

A further reason for investigating the dependence of the properties of the glass on the cooling rate originates from those computer simulations in which a relatively realistic type of model is used in the calculation with the goal to simulate *real* glass formers, such as SiO_2 . In these simulations the quality of the applied model is in most cases judged by its ability to reproduce some experimentally determined quantities, such as the temperature dependence of the density, radial distribution functions or bond angle distributions functions⁸. Before such a judgement can be made, however, it is necessary to see how the properties of the glass, as determined from a computer simulation which involves cooling rates that can be more than ten orders of magnitude larger than the ones in real laboratory experiments, are affected by these high cooling rates. It might well be, that a discrepancy between the prediction of a model and the experimental data is not due to the inadequacy of the model, but due to the too high cooling rate with which the glass on the computer was produced. Thus it is important to separate these two possible sources of the discrepancy, and investigating the cooling rate dependence of the properties of the glass is one possible way to do this.

In the present paper we investigate the dependence of the glass transition phenomenon and the properties of the resulting glass on the cooling rate. The system we use is a binary mixture of Lennard-Jones particles, since this is a prototype of a simple glass former. The goal of this work is to show that for this system there are significant dependencies of the details of the glass transition and of the macroscopic and microscopic properties of the glass on the cooling rate. We emphasize, however, that we do not address the question of what the underlying microscopic mechanism for the glass transition is—a question that has in recent years been the focus of much theoretical effort and many computer simulations—rather we investigate how the experimentally observed cooling rate dependencies of *macroscopic* properties of glass are reflected in the cooling rate dependence of the *microscopic* properties of glass and attempt to relate these two dependencies to each other, independent of the exact mechanism for the glass transition.

The rest of the paper is organized as follows. In Sec. II we introduce our model and give some of the details of the simulation. In the first part of Sec. III we present our results regarding the cooling rate dependence of the glass transition and in the second part of that section we give the results of the cooling rate dependence of the resulting glass. In Sec. IV we then summarize and discuss these results.

II. MODEL AND DETAILS OF THE SIMULATION

The system we investigate is a binary mixture of particles, subsequently called type *A* and type *B*, each of them having the same mass m . The interaction between two par-

ticles of type α and β ($\alpha, \beta \in \{A, B\}$) is given by a Lennard-Jones potential, i.e. $V_{\alpha\beta}(r) = 4\epsilon_{\alpha\beta}[(\sigma_{\alpha\beta}/r)^{12} - (\sigma_{\alpha\beta}/r)^6]$. The parameters $\epsilon_{\alpha\beta}$ and $\sigma_{\alpha\beta}$ were chosen to have the following values: $\sigma_{AA} = 1.0$, $\epsilon_{AA} = 1.0$, $\sigma_{AB} = 0.8$, $\epsilon_{AB} = 1.5$, $\sigma_{BB} = 0.88$, and $\epsilon_{BB} = 0.5$. In order to decrease the computational burden this potential was truncated and shifted at $r = 2.5\sigma_{\alpha\beta}$.

The model presented has already been used to investigate the dynamics of strongly supercooled liquids.⁹ From these previous investigations it is known that this system is a good glass former, in that it is not prone to crystallization, even if the system is cooled very slowly. Therefore this system is a good model for investigating the dependencies of various properties of the glass on the cooling rate. We also mention that this potential is very similar to the one proposed by Weber and Stillinger for the $\text{Ni}_{80}\text{P}_{20}$ alloy.¹⁰ However, since in our study the masses of the two particles are the same, whereas in the Ni–P system the ratio should be approximately 2:1, we expect that the microscopic structure of our model is similar to the $\text{Ni}_{80}\text{P}_{20}$ system, but that the dynamics is different.

In the following all results are given in reduced units. The unit of length is σ_{AA} , the unit of energy is ϵ_{AA} and the unit of time is $(m\sigma_{AA}^2/48\epsilon_{AA})^{1/2}$. For the case of the $\text{Ni}_{80}\text{P}_{20}$ system these units correspond to approximately 2.22 Å, 933 $k_B\text{K}$ and 9.0×10^{-14} s. In order to allow the investigation of the dependence of the density of the glass on the cooling rate and the computation of the specific heat at constant pressure, the simulations were performed at a constant pressure p_{ext} . This was done by using the algorithm proposed by Andersen.¹¹ The external pressure p_{ext} was chosen to be 1.0 and we used the value of 0.05 for M , the mass of the piston. This value of M is sufficiently small to allow the volume of the system to relax quickly when the temperature of the system is changed and the system therefore contracts. However, as we will see below, for the fastest cooling rates the inertia of the volume variable still affects the results. We will come back to this point in the next section.

In order to simulate the cooling process we proceeded as follows. The system was equilibrated in an NpT -ensemble at a high temperature T_i which was for most cooling processes chosen to be 2.0 (see below for a modification of this value). At this temperature the relaxation times are short and thus equilibration is fast. After this equilibration period we began with the cooling process. For this we integrated the equations of motion with the velocity form of the Verlet algorithm, using a time step of 0.02. Every 150 time steps the velocities of all the particles were replaced by new velocities which were drawn from a Boltzmann distribution corresponding to the temperature T_b of the heat bath. The temperature of this bath was decreased linearly in time, i.e., $T_b(t) = T_i - \gamma t$, where γ is the cooling rate. This cooling process was continued until the temperature of the bath was zero, i.e., for a time T_i/γ , which means that for the smallest cooling rate ($\gamma = 3.125 \times 10^{-6}$) the length of the run was 8×10^6 time steps. Using the multidimensional conjugate gradient method,¹² the coordinates of the particles as well as the volume were subsequently allowed to relax to the nearest local

minimum of the potential energy hypersurface. It should be mentioned that an equivalent way to relax the configurations would have been to continue the molecular dynamics simulation at $T_b=0$ for a *long* time and that the only reason for using the conjugate gradient method was computational efficiency.

The cooling rates we investigated were: $\gamma=0.02$, 0.01 , 0.005 , 0.0025 , 0.001 , 5.0×10^{-4} , 2.5×10^{-4} , 1.0×10^{-4} , 5.0×10^{-5} , 2.5×10^{-5} , 1.25×10^{-5} , 6.25×10^{-6} , and 3.125×10^{-6} . The number of *A* particles was 800 and the one for the *B* particles was 200. In order to test for finite size effects we also did some runs for a system twice as large. In order to decrease the error bars of our results we averaged the results for each value of γ over ten independent runs, each of which was equilibrated at $T_i=2.0$ for 2000 time units. Since at the smallest cooling rate each of these runs took about 280 hours of CPU time on an IBM RS6000/375 it is today probably not possible to investigate a range of cooling rates that is significantly larger than the one investigated here.

Finally we remark on the choice of the starting temperature T_i for the cooling process. It can be expected that for a given cooling rate γ the temperature $T_g(\gamma)$ at which the system falls out of equilibrium, and hence the properties of the resulting glass, is independent of the starting temperature T_i , as long as T_i is sufficiently above T_g , or, to put it differently, that the time constant of the cooling, $[(-dT/dt)/T_i]^{-1}=1/\gamma T_i$, is larger than the intrinsic relaxation time of the system at the temperature T_i . In order to save computer time we therefore chose for the small values of γ a value for T_i which was lower than the corresponding value for large values of γ . In particular we chose T_i to be 2.0 for $\gamma \geq 1.0 \times 10^{-4}$, equal to 1.0 for $\gamma = 5.0 \times 10^{-5}$, 2.5×10^{-5} , 1.25×10^{-5} and equal to 0.5 for the two smallest values of γ . In all cases we made sure that the value of the glass transition temperature is indeed smaller than T_i , which was done by investigating the temperature dependence of the enthalpy and the density (see below for details).

More information regarding the details of the simulation can be found in Ref. 13.

III. RESULTS

In this section we will report the results of our simulation. In the first subsection we will discuss the cooling rate dependence of the system *during* the cooling process, i.e., look at the system at finite temperatures, and hence investigate the details of the *glass transition*. In the second subsection we will present the results on the cooling rate dependence of the so obtained *glass* at $T=0$.

A. Finite temperatures

In this subsection we will investigate the properties of the system *during* the cooling process and see how these properties depend on the cooling rate. One of the simplest quantities one can investigate is the enthalpy $H(T_b) = E_{\text{kin}} + E_{\text{pot}} + p_{\text{ext}}V + M\dot{V}^2/2$, where V is the volume of the system. This quantity has been studied in many previous computer simulations and it was found that on lowering

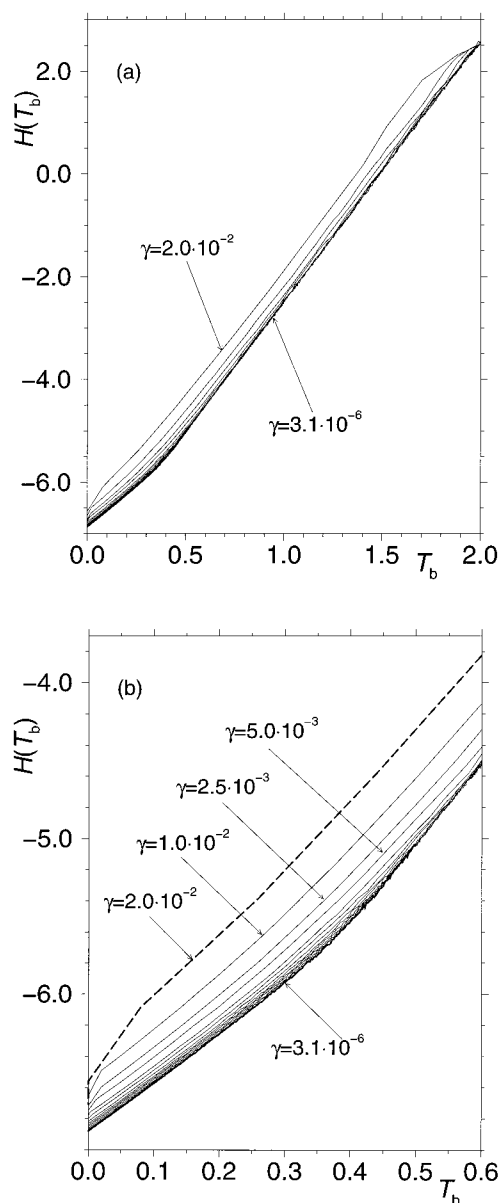


FIG. 1. Enthalpy H of the system versus T_b , the temperature of the heat bath, for all cooling rates investigated. (a) Full range of temperature. (b) Enlargement of the glass transition region. The solid and dashed bold curves are the smallest and largest cooling rates, respectively.

the temperature a noticeable bend in $H(T_b)$ occurs at the temperature at which the system falls out of equilibrium. Therefore, the temperature at which this bend occurs is usually identified with the glass transition temperature T_g .

In Fig. 1 we show the enthalpy H as a function of T_b , the temperature of the bath, for all cooling rates investigated. We see [Fig. 1(a)] that at high temperatures the curves for the intermediate and small cooling rates (bottom curves) fall onto a master curve. This master curve is given by the equilibrium value of the enthalpy of the system in its (supercooled) liquidlike state, i.e., by the curve one would obtain for an infinitely small cooling rate. For a given cooling rate the enthalpy of the system will be given by this equilibrium curve provided that the temperature of the system is high

enough to allow it to equilibrate before a significant change in temperature, due to the cooling, has happened. If this condition is violated the system will fall out of equilibrium, and start to show a solid-like behavior, which is reflected by the bending of the curve for the enthalpy. Thus the system has undergone a glass transition. We therefore expect that the temperature T_g at which this transition happens is smaller the lower the cooling rate is. That this is indeed the case is shown in Fig. 1(b) in which we show the temperature region in which the glass transition occurs on an enlarged scale. We recognize that the smaller the cooling rate is (curves at the bottom) the later these curves split off from the liquidus curve. Later we will investigate this phenomenon more quantitatively.

From Fig. 1(a) we also recognize that for the fastest cooling rates (top curves) the system falls out of equilibrium already at the starting temperature T_i . These cooling rates are so large, that it is no longer appropriate to see the cooling as a process which ultimately forces the system to fall out of equilibrium because its relaxation times exceed the time scale of the simulation, but rather as similar to a steepest descent procedure of the system with respect to the enthalpy. Furthermore it is likely that the exact form of these curves will depend on the details of the cooling process, such as the frequency with which the system is coupled to the heat bath or the mass of the piston. Therefore we can expect that for such large cooling rates the temperature dependence of various quantities is qualitatively different from the one for smaller cooling rates and the fact that the curves for the enthalpy split off from the master curve already at T_i is an example for such a different type of behavior.

The just presented temperature dependence for the enthalpy is very similar to the one found for the density ρ . The temperature dependence of ρ (see Fig. 2) shows that $\rho(T_b)$ has, similar to $H(T_b)$, a bend in the vicinity of $T_b \approx 0.4$ and that the curves corresponding to the various values of γ split off from the liquidus curve at a temperature that is lower the smaller γ is. We also note that for this system the temperature dependence of the density is a monotonous function of temperature which will allow us later to define in a simple way a glass transition temperature. It has to be remarked that this is not a universal property, since other systems, such as SiO_2 , show an anomaly in the density and thus make the extraction of a glass transition temperature from the density much more difficult¹⁴. We also recognize from the inset in Fig. 2, that for this system the density varies by more than a factor of two when the temperature is changed from $T=2.0$ to $T=0$, which is also in strong contrast with the case of the network glass former SiO_2 .¹⁴

By differentiating the enthalpy with respect to the temperature we obtain c_p , the specific heat at constant pressure. Since our data for $H(T_b)$ was a bit too noisy to compute its derivative directly from a difference quotient, we approximated $H(T_b)$ by a spline under tension¹⁵ and then determined c_p by taking the difference quotient of this spline. In Fig. 3 we show the so obtained curves for c_p for all cooling rates investigated. We see [Fig. 3(a)] that at high temperatures and very fast cooling rates c_p drops from a value of

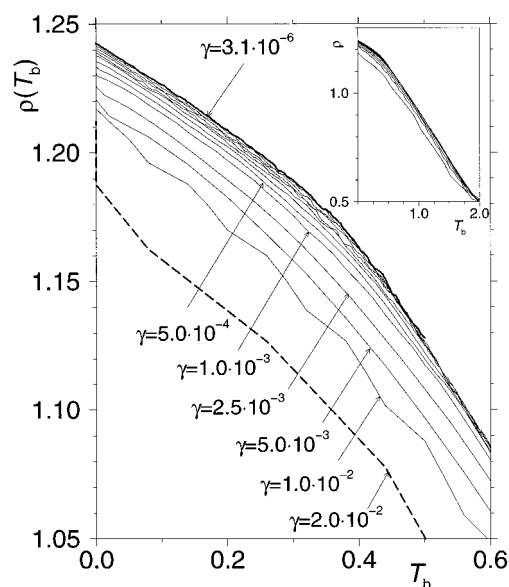


FIG. 2. Density ρ of the system versus T_b , the temperature of the heat bath, for all cooling rates investigated. Main figure: The glass transition region. The solid and dashed bold curves are the smallest and largest cooling rates, respectively. Inset: Full range of temperature.

around 5 to significantly smaller values when the temperature is increased. This decrease is again a signature that for these large cooling rates the system falls out of equilibrium immediately after the cooling process is started. Thus this decrease should not be seen as the generic behavior of c_p for intermediate and small cooling rates. Rather we see that for such values of γ , c_p is almost independent of T_b for T_b larger than 0.8. Only when the temperature is decreased to approximately 0.5 do we see that the value of c_p starts to drop from a value around 5.0 to a value around 3.0, the value expected for a classical harmonic system. We also recognize that even at these low temperatures the values for c_p for the fast cooling rates are considerably larger than the harmonic value 3.0. This shows that for these fast quenches the system behaves very anharmonically even at very low temperatures.

In order to more clearly see the dependence of c_p on the cooling rate we show in Fig. 3(b) the temperature range in which c_p shows the strong decrease on an expanded scale. We recognize that the temperature range in which this drop occurs is identical to the temperature range in which the bend is observed in the enthalpy and the density (see Figs. 1 and 2) and thus is related to the glass transition.

From Fig. 3(b) we recognize that the drop of the curves becomes sharper the smaller the cooling rate is. Thus we find that the glass transition becomes more pronounced with decreasing cooling rate, in accordance with the simple argument put forward by Angell *et al.*¹⁶ which says that, since the relaxation times are a strong function of temperature, e.g., of Arrhenius or Vogel–Fulcher type, the temperature difference $T_2 - T_1$ for which the relaxation times change by, say, a factor of 100, i.e., $\tau(T_1)/\tau(T_2) = 100$, decreases with decreasing T_1 . Since we have seen that the glass transition temperature T_g decreases with decreasing γ , it thus follows

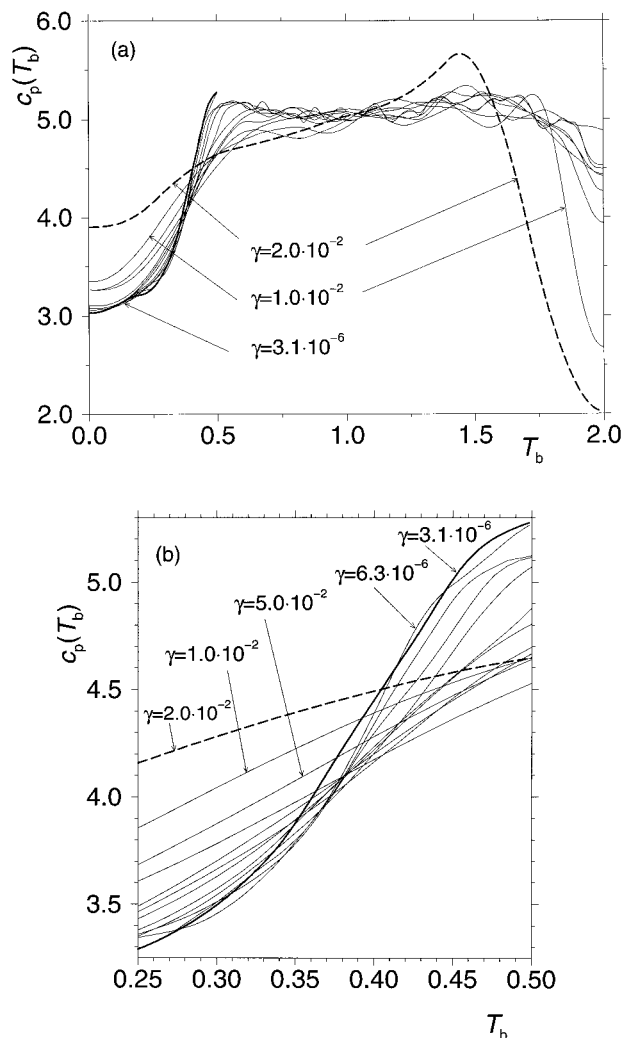


FIG. 3. Specific heat at constant pressure versus T_b for all cooling rates investigated. The solid and dashed bold curves are the smallest and largest cooling rates, respectively. (a) Full range of temperature. (b) Enlargement of the glass transition region.

that the transition happens in a temperature range $T_1 \leq T_g \leq T_2$ which becomes narrower the smaller the cooling rate is.

A qualitatively similar behavior to the cooling rate dependence of c_p is found for the cooling rate dependence of the thermal expansion coefficient $\alpha_p(T_b)$. This quantity is given by $\alpha_p(T_b) = V^{-1} dV(T_b)/dT_b|_p$ and is shown in Fig. 4 for all cooling rates investigated. To compute the derivative we again made use of splines under tension. The drop in α_p at high temperatures for large values of γ should again be viewed as the atypical behavior of α_p for very large cooling rates. For intermediate and small cooling rates we see that α_p shows an almost linear dependence on temperature until it shows a rather sudden drop when the glass transition temperature is reached. As in the case of the specific heat this drop becomes sharper with decreasing cooling rate. Thus we see also for this quantity that the glass transition becomes more pronounced the smaller the cooling rate is. However, it is clear that even for our smallest cooling rate the glass tran-

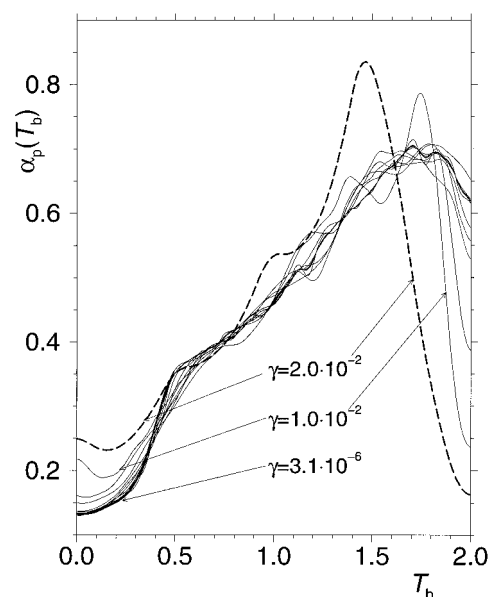


FIG. 4. Thermal expansion coefficient α_p versus T_b for all cooling rates investigated. The solid and dashed bold curves are the smallest and largest cooling rates, respectively.

sition is still smeared out over a relatively large temperature range, unlike the real experiment at much smaller cooling rates.

From Figs. 1 and 2 we see that the temperature at which the curve for a given value of the cooling rate splits off from the liquidlike branch decreases with decreasing γ . This means that the glass transition temperature T_g decreases with decreasing cooling rate. In order to investigate this effect in more quantitative terms we use the concept of the “fictive temperature” as introduced long ago by Tool and Eichlin.¹⁷ This concept is founded on two observations: The first is that at high temperatures the temperature dependence of most bulk properties of the system is independent of the cooling rate, i.e., the curves for the different cooling rates fall onto a master curve, as we see it, e.g., in Figs. 1 and 2. This master curve can thus be approximated by a low order polynomial and therefore extrapolated to low temperatures. The second observation is, that the low temperature behavior of these bulk properties, is, apart from an additive constant, independent of the cooling rate (see, e.g., Figs. 1 and 2). The physical reason for this is that the temperature dependence of such bulk quantities is not very sensitive to the details of the microscopic structure of the glass, which themselves are dependent on the cooling rate, as we will see below. Therefore also this low temperature branch can be approximated by a low order polynomial and thus extrapolated to higher temperatures. The point where the extrapolations of the extrapolated curves at high and low temperatures intersect is the fictive temperature, which in this work we will call the glass transition temperature T_g . Note that this construction is only possible if the curves actually fall onto a master curve at high temperatures. Since this is not the case for the fastest cooling rates investigated here, we determined T_g only for the intermediate and small cooling rates, i.e., $\gamma \leq 0.005$.

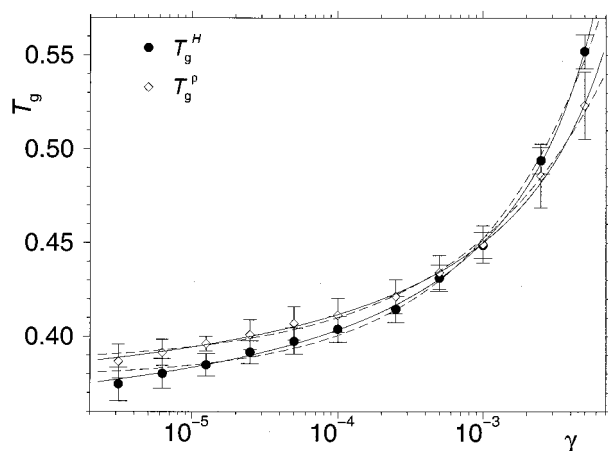


FIG. 5. Glass transition temperature T_g , as determined from the enthalpy (circles) and the density (diamonds), versus the cooling rate. The solid and dashed lines are fits with the functional forms given in Eq. (1) and Eq. (2), respectively.

In order to determine the low temperature master curve we shifted the curves for the different values of γ vertically by a γ dependent amount until the curves lay on a master curve in the temperature range $0 \leq T_b \leq 0.2$. The so obtained master curve was fitted in this temperature range with a quadratic polynomial. (We note that a linear function, as has been used in several other investigations, did not give a good fit to our low temperature data.) The master curve for the high temperature data in the range $0.6 \leq T_b \leq 0.8$ was fitted well by a linear function in the case of the enthalpy, whereas a quadratic polynomial was needed in the case of the density.

In Fig. 5 we present the glass transition temperatures, as determined by the procedure described above, as a function of the cooling rate. The error bars are estimated from the uncertainty in the determination of the intersection points of the extrapolated curves. We see that, as expected, T_g decreases with decreasing cooling rate. We also recognize that the values of T_g as determined from the enthalpy are not exactly the same as the ones as determined from the density, in that, e.g., for not too large a cooling rate, the former are systematically lower than the latter. At the moment we are not able to say whether this behavior has some real underlying physical reason or whether it just reflects some systematic error in our determination of T_g . It is not implausible at all, that the glass transition temperature depends on the quantity investigated but it is also possible that such a dependence vanishes at very small cooling rates, where the glass transition is much sharper than in the present case.

The dependence of T_g on the cooling rate has also been determined in experiments¹. It was found that the functional form

$$T_g(\gamma) = T_0 - \frac{B}{\log(A\gamma)} \quad (1)$$

is able to give a satisfactory fit to the data when γ is varied over 3 decades. The functional form of Eq. (1) can be rationalized by assuming that the relaxation time $\tau(T)$ of the

system shows a Vogel–Fulcher dependence on temperature, i.e., $\tau(T) = A \exp(B/(T-T_0))$ and by assuming that the system falls out of equilibrium at that temperature $T_g(\gamma)$ where the relaxation time is of the order of the inverse of the cooling rate, i.e. $\tau(T_g(\gamma)) \propto \gamma^{-1}$. In Ref. 9 it was shown that, at constant volume, the temperature dependence of the relaxation times of the system is also fitted very well by a power law, a functional form proposed by the so-called mode-coupling theory.¹⁸ If we use this functional form for τ , i.e., $\tau(T) = A/(T-T_c)^\delta$, we expect that T_g depends on γ via

$$T_g(\gamma) = T_c + (A\gamma)^{1/\delta}. \quad (2)$$

Also included in Fig. 5 are fits to the data with the functional forms given by Eq. (1) (solid curves) and Eq. (2) (dashed curves). We see that both fits are able to represent the data very well. The temperature T_0 from Eq. (1), i.e., the glass transition temperature for an infinitely slow cooling process, is 0.334 and 0.348 for the enthalpy and the density, respectively and the corresponding values for T_c from Eq. (2) are 0.378 and 0.386, respectively. Also in this case it is not clear whether the difference between the values of T_0 (or T_c) for H and ρ has some underlying physical reason or whether it is just a systematic error in the way we determined $T_g(\gamma)$.

We also note that the estimated value for T_c is significantly larger than the one estimated for T_0 which is in accordance with experiments where it is found that $T_c \geq T_0$.

B. Zero temperatures

After having discussed in the preceding subsection the cooling rate dependence of various quantities at *finite* temperatures we now investigate how the properties of the glass at *zero* temperature depend on the cooling rate.

We have seen in Fig. 1 that the smaller the cooling rate is the lower is the temperature at which the curve for the corresponding γ splits off from the liquidus curve. Thus we expect that the value of the enthalpy at zero temperature will depend on γ . That this is indeed the case is shown in Fig. 6, where we plot H_f , the final enthalpy after the quench (and the subsequent relaxation of the system, see Sec. II) as a function of γ . As expected, we find that H_f decreases with decreasing cooling rate. We see that the dependence of H_f on γ becomes stronger when we change γ from small values to intermediate and large values. For very large values the dependence becomes, however, weaker again. This can be understood by noticing, that for such large values of γ the cooling process is very similar to a steepest descent procedure and that therefore in the limit $\gamma \rightarrow \infty$ the dependence of the final state on the cooling rate vanishes (and is independent of the details of the cooling process).

Also included in Fig. 6 is the result of a cooling process for $\gamma = 5.0 \times 10^{-5}$ for a system size of 2000 particles. This point was generated by averaging over 5 different initial configurations and the goal of this “experiment” was to see whether our results are affected in some way by finite size effect. Since the result for the system sizes $N=1000$ and $N=2000$ are the same to within the error bars, we conclude

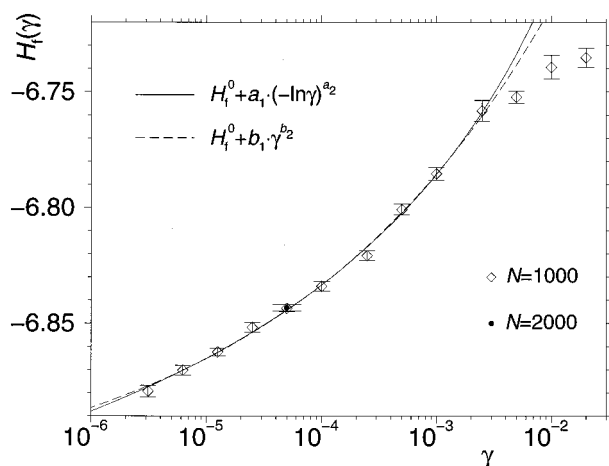


FIG. 6. H_f , the value of the enthalpy after the quench, as a function of the cooling rate for the system of 1000 particles (open symbols) and the system of 2000 particles (solid symbol). Also included are the results of fits with the functional forms given in Eq. (3) (dashed curve) and Eq. (4) (solid curve).

that, for the types of questions investigated in this work, finite size effects are not important for the model studied here.

Since the system will try to decrease its enthalpy during the quench, the cooling process can also be viewed as an optimization process in which the system tries to minimize a cost function, i.e., the enthalpy. The dependence of the value of the cost function on the amount of time spent to find this value has been the subject of quite a few earlier investigations. A discussion of some of this previous work can be found in Ref. 19 (see also Refs. 4, 20, and 21).

In the just mentioned investigations dealing with cooling or optimization processes it has been proposed that the dependence of the cost function, i.e., in our case the enthalpy, on the cooling rate is given by a power law or by a logarithmic dependence, i.e.,

$$H_f(\gamma) = H_f^0 + a_1 \gamma^{a_2} \quad (3)$$

or

$$H_f(\gamma) = H_f^0 + b_1 (-\log \gamma)^{b_2}, \quad (4)$$

where H_f^0 , a_i and b_i are fit parameters.²⁰ Therefore we have tried to fit our data for $H_f(\gamma)$ with these functional forms and the best fits are included in Fig. 6 as well. Since the functional forms can be expected to hold only for small cooling rates, the three largest cooling rates were not included in the fitting procedure. These cooling rates are the ones for which the dependence of H_f on γ becomes weak again, i.e. for which the cooling process is similar to a steepest descent. Figure 6 shows that *both* functional forms are able to fit the data very well. Thus within the accuracy of our data and the cooling range investigated it is not possible to decide which functional form, if any, is the correct one.

We also notice that for cooling rates $\gamma \leq 2.5 \times 10^{-4}$ the data points for H_f lie, within the accuracy of our data, on a straight line. It is clear that such a functional dependence of H_f on γ cannot be valid for arbitrarily small cooling rates,

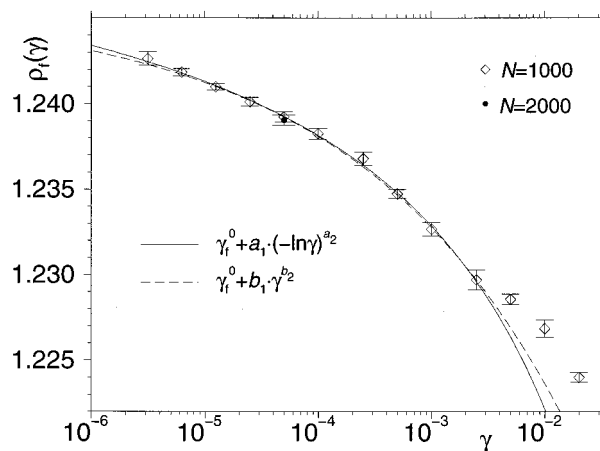


FIG. 7. ρ_f , the value of the density after the quench, as a function of the cooling rate for the system of 1000 particles (open symbols) and the system of 2000 particles (solid symbol). Also included are the results of fits with the functional forms given in Eq. (3) (dashed curve) and Eq. (4) (solid curve).

since this would lead to arbitrarily low values of H_f for sufficiently small γ . Thus if there actually exists a regime for which there is a linear dependence of H_f on the logarithm of γ , there also must exist at even smaller values of γ a further regime, in which H_f shows the real asymptotic dependence on γ . However, this regime is currently outside of our computational possibilities.

In Fig. 3(a) we have shown that for large cooling rates the system behaves very anharmonically even at low temperatures. Now we find that for these cooling rates the enthalpy of the local minimum in which the systems ends at $T_b=0$ is relatively large. Thus we conclude that for this system the hypersurface of the enthalpy has the property that on average its shape is very anharmonic when the enthalpy is large and relatively harmonic when the enthalpy is small.

Similar to the enthalpy we have found that also ρ_f , the density of the system after the quench, shows a small but noticeable dependence on the cooling rate. The results are shown in Fig. 7. Note that a change of γ by about four orders of magnitude leads to a change in ρ_f of only 2%, a figure which is comparable to the one found in experiments (although at vastly slower cooling rates).¹ The smallness of the effect shows that it is necessary to vary the cooling rate over an extensive range and to use system sizes that are not too small in order to obtain results of sufficient statistical accuracy.

Also in the case of ρ_f we found that, for not too large values of γ , the data can be fitted by the two functional forms given by Eqs. (3) and (4) equally well. The densities ρ_f^0 are 1.246 and 1.253 for the power-law and logarithmic functional forms, respectively. Furthermore we see, that, as in the case of the enthalpy, also for this quantity finite size effects are not important and that the data points for intermediate and small values of γ lie on a straight line, thus indicating the possibility of a further type of relaxation regime at even lower values of γ .

Since we have now seen that *bulk* quantities such as the

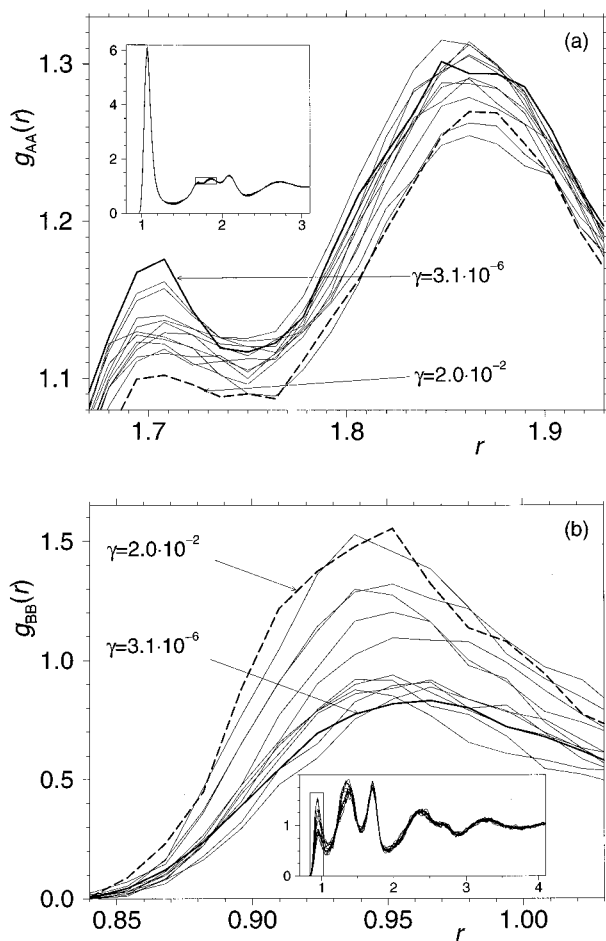


FIG. 8. The radial distribution function at $T=0$ for all cooling rates investigated. The solid and dashed bold line correspond to the slowest and fastest cooling rates, respectively. (a) $g_{AA}(r)$, (b) $g_{BB}(r)$.

enthalpy and the density show a dependence on the cooling rate, it is interesting to investigate how these dependencies can be understood from a microscopic point of view. Therefore we will investigate in the following how the *microscopic* structure of the glass changes when the cooling rate is varied. In Fig. 8 we show the radial distribution functions $g_{AA}(r)$ and $g_{BB}(r)$ for the AA and BB correlations.²² The results for $g_{AB}(r)$ are similar to the ones for $g_{AA}(r)$. The inset in Fig. 8(a) shows that the overall form of $g_{AA}(r)$ does not show a *strong* dependence on γ . A closer investigation of the first nearest neighbor peak showed that for the smallest cooling rate its height is about 2% higher than the one for the largest cooling rate.¹³ A somewhat stronger dependence can be observed in the second nearest neighbor peak, part of which is shown in the main figure of Fig. 8(a). We recognize that the curve for the slowest cooling rate (solid bold line) shows more pronounced peaks than the curve for the fastest cooling rate (dashed bold line). Thus we conclude that the local order of the system, as measured by $g_{AA}(r)$, becomes more pronounced with decreasing cooling rate.

A similar behavior as the one observed for $g_{AA}(r)$ is found for $g_{BB}(r)$ [Fig. 8(b)]. However, in this case the height of the *first* nearest neighbor peak shows a relatively strong

dependence on the cooling rate. We see that in this case the height of this peak *decreases* with decreasing cooling rate. This behavior can be understood by remembering that ϵ_{BB} , the interaction energy of the Lennard-Jones potential between two B particles, is only 0.5, as compared to 1.5 for ϵ_{AB} . Therefore the system will try to avoid having two B particles as nearest neighbors, and to have A and B particles as nearest neighbors instead, and it will manage to do this better the more time it is given to do so, i.e., the smaller the cooling rate is.²³ However, from the figure we also recognize that the height of the first nearest neighbor peak decreases when the cooling rate is decreased from very large values to intermediate values, but that for even smaller cooling rates the γ -dependence of the height is much weaker, if it exists at all. This indicates that the above mentioned driving force for decreasing the peak is no longer effective for intermediate and small cooling rates and that therefore a different mechanism must exist in order to explain the decrease of the enthalpy or the density.

Having the information on the various radial distribution functions we can now investigate the dependence of the different types of coordination numbers of the particles on the cooling rate. We define the coordination number z of a particle of type α to be the number of particles of type β that are closer to the first particle than $r_{\min}^{\alpha\beta}$, the location of the first minimum in $g_{\alpha\beta}(r)$. We have found that the value of $r_{\min}^{\alpha\beta}$ depends only weakly on the cooling rate¹³ and thus we have chosen the following, γ -independent, values for $r_{\min}^{\alpha\beta}$: $r_{\min}^{AA}=1.4$, $r_{\min}^{AB}=1.2$, and $r_{\min}^{BB}=1.07$.

In Fig. 9 we show the γ dependence of $P_{\alpha\beta}$, the probability that a particle of type α has z nearest neighbors of type β for various values of z . We see that the curves for the AA pairs, Fig. 9(a), for $z=12$ and $z=13$ increase with decreasing γ , that the curve for $z=10$ shows a decreasing trend and that the curve for $z=11$ is essentially independent of γ . We recognize that the changes that take place in the distribution of the coordination number are relatively small, i.e., less than 10%, when the two particles are of type A. This is not the case for the BA and BB pairs as is shown by Figs. 9(b) and 9(c). Here we see that the change in the coordination number can be as much as 50% [$z=7$ and $z=9$ in Fig. 9(b)]. Furthermore we find that the coordination numbers for BB pairs for $z=0$ and $z=1$ increase and decrease, respectively, with decreasing cooling rate [Fig. 9(c)]. This observation is in accordance with the comments we made in the context of Fig. 8(b), where we found that the height of the first nearest neighbor peak in the BB correlation function is decreasing with decreasing γ . We also see in Fig. 9(c) that for values of γ less than 10^{-4} , the value of P_{BB} for $z=0$ is essentially independent of γ , this is in accordance with the comments made before. We also mention that from Fig. 9(a) one should *not* conclude that, since the curve P_{AA} for $z=12$ shows an increasing trend, for very small cooling rates the *total* number of nearest neighbor particles of an A particle is 12. What is shown in the figure is just the number of nearest A particles, thus the B neighbors are not taken into account. As we will show below the most frequent values of the total coordination number for the A particles is 13 and

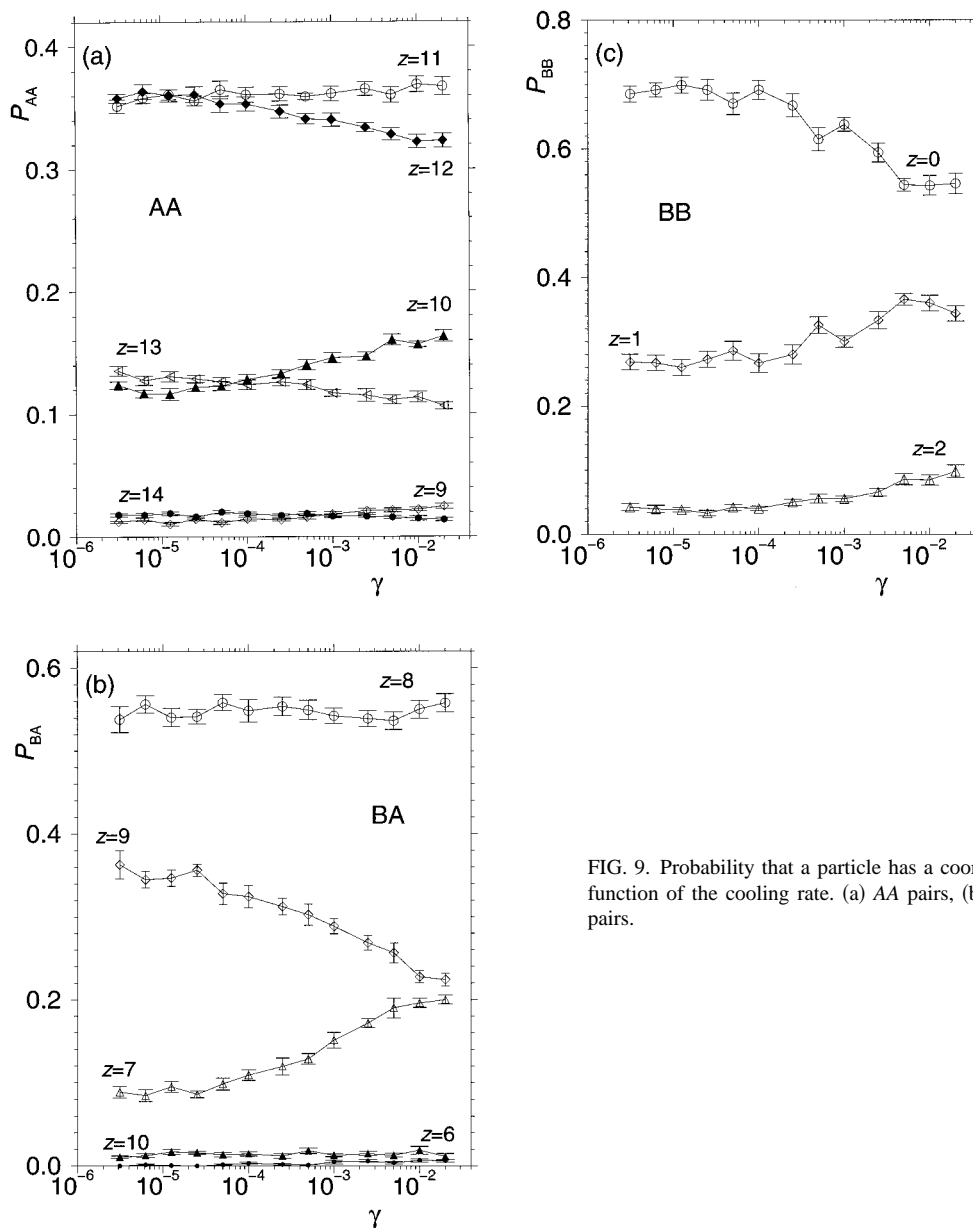


FIG. 9. Probability that a particle has a coordination number z as a function of the cooling rate. (a) AA pairs, (b) BA pairs, and (c) BB pairs.

14. This is different from the results one might expect for a one-component system, where at low temperatures particles tend to pack locally in an icosahedral structure, thus leading to a coordination number of 12. Since in our case we have a mixture of large and small particles it can thus be expected that the value of the most frequent coordination number is larger than 12 and below we will show that this is indeed the case.²⁴ We also note that our finding that icosahedra are not very frequent does not contradict the results of Jónsson and Andersen for a similar Lennard-Jones system.²⁵ These authors showed that with decreasing temperature particles form pairs which are embedded in a local structure that *can* be considered as part of an icosahedron. However, the temperature dependence of the frequency with which *icosahedra* occur was not investigated and thus their finding is consistent with our results.

The fact that the nearest neighbor particles of an A par-

ticle do not form an icosahedron is also supported by the form of the bond–bond angle distribution function. Here we define a bond as the line segment connecting two neighboring particles and a bond–bond angle as the angle between two bonds which are connected to a common particle. In Fig. 10 we show this distribution function for the case of three A particles. Note that if the local structure of the particles would be a perfect icosahedron we would have only contributions at angles 63.4° and 116.6° . We see (inset in Fig. 10), that the distribution function indeed shows maxima close to the mentioned angles, but that the maxima are at 58.5° and 110° , respectively, and that the peaks are very broad, thus showing that the local structure is clearly not a perfect icosahedron. The overall form of the distribution function shows only a small dependence on the cooling rate, the most pronounced effect seems to be that the height of the peak near 60° increases and shows the tendency to shift its position to

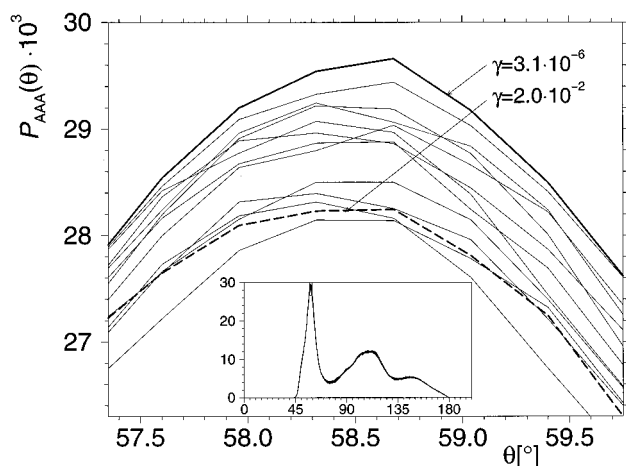


FIG. 10. Distribution of the bond–bond angle between three A particles for all cooling rates investigated. Inset: The whole distribution. Main figure: Enlargement of the peak around 60° . The solid and dashed bold lines correspond to the fastest and slowest cooling rate, respectively.

larger values of the angle with decreasing cooling rate (main figure). The smallness of these effects is in stark contrast with our findings for the network glass former SiO_2 for which we found a strong dependence of the distribution function for the angles on the cooling rate¹⁴.

Since we have now evidence that the arrangement of the particles making up the nearest neighbor shell of the A particles is not similar to an icosahedron, we now investigate what the nature of this arrangement really is. Furthermore we will also try to understand, what the underlying reason for the cooling rate dependence of H_f and ρ_f is. In order to do this we introduce the notion of a “cluster.” We define a cluster of particles as the collection of particles given by a central particle and the particles of its nearest neighbor shell (computed by using the distances $r_{\min}^{\alpha\beta}$). We say that a cluster is of type $\alpha_{\mu,\nu}$, if the central particle is of type $\alpha \in \{A, B\}$ and if it has μ nearest neighbors, ν of which are of type B . Note that this definition of a cluster can be viewed as a first step of a whole hierarchy of definitions of clusters in which, e.g., one defines clusters as the collection of particles that are within the first or first two nearest neighbor shell(s), etc., and specifying how many particles of each type are in any given shell. However, in order to avoid complicating the analysis of the data too much we restrict ourselves to this simplest kind of cluster definition.

We define the energy of a cluster to be given by the sum of all pairwise interactions between any two members of the cluster and will denote this energy by E_c . The dependence of E_c on the cooling rate is shown in Fig. 11 for various types of clusters. In order not to crowd the figure too much, we show only a representative selection of the types of clusters we found. (More curves can be found in Fig. 2 of Ref. 26). The dependence of E_c on γ for the types of clusters not shown is very similar to the one of the types of clusters shown. The following observations can be made: (1) For all types of clusters E_c decreases with decreasing cooling rate. A variation of 4 decades in γ gives rise to a decrease of

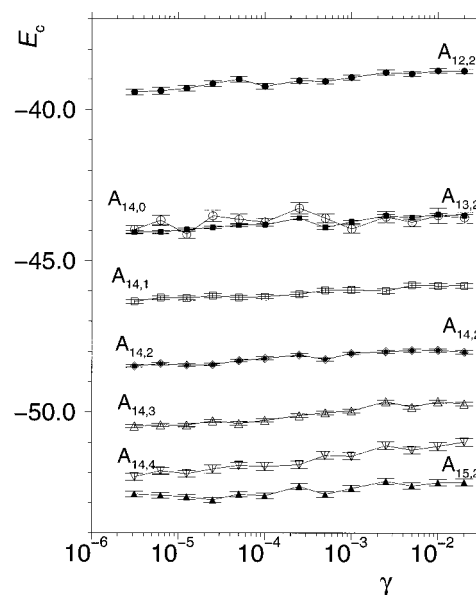


FIG. 11. E_c , the energy of a cluster as a function of the cooling rate for selected cluster types. Note that the energy of the cluster of type $A_{\mu,\nu}$ decreases with increasing μ when ν is held fixed (filled symbols) and that E_c also decreases with increasing ν when μ is held fixed (open symbols).

about 1%. (2) For a given cooling rate the difference of E_c between the different types of clusters is usually much larger than 1%. (3) For a given number of B particles in a cluster, E_c decreases with increasing number of A particles in the cluster [as exemplified in the figure by the clusters $A_{\mu,2}$ (solid symbols)]. (4) For a given total number of particles in the cluster, E_c decreases with increasing number of B particles (as exemplified in the figure by the clusters $A_{14,\nu}$ (open symbols)). Although we have shown here only the dependence of E_c on γ for clusters of type $A_{\mu,\nu}$ similar results also hold true for clusters of the type $B_{\mu,\nu}$.¹³

Since for each type of cluster a variation of γ by four decades gives rise to a change in E_c on the order of one percent and since the change of the enthalpy, which is related to the sum of the energy of the clusters, is also on the order of 1%–2%, one might conclude that the change of the enthalpy can be rationalized solely by the change of the energy of the clusters. Before one can draw this conclusion one has, however, to see whether the distribution of the frequency of the different types of clusters is not also changing with the cooling rate. In Fig. 12 we show the probability $P_{\alpha_{\mu,\nu}}$ that a cluster is of type $\alpha_{\mu,\nu}$ as a function of γ . In order not to crowd the two figures too much, we show only those curves for which this probability is not too small. We recognize that there are clusters for which this probability is essentially independent of γ , such as, e.g., cluster $A_{13,2}$ in Fig. 12(a), and that there are quite a few clusters for which this probability changes by more than 10% (all the clusters that are marked by symbols). Since we have seen from Fig. 11 that the difference between the energy of different clusters is usually much larger than 1%–2%, the amount of energy a particular cluster changes when γ is changed by four decades, we thus

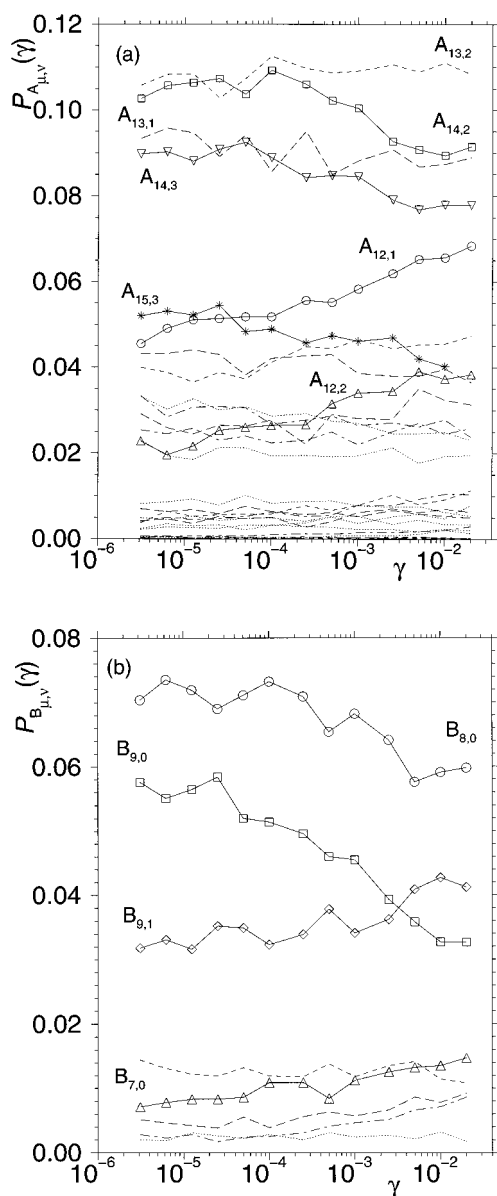


FIG. 12. Probability to find a cluster of a given type as a function of γ . Only the curves for the clusters showing a noticeable change as a function of γ (marked with symbols) or that are very frequent are labeled. (a) Clusters around A particles. (b) Clusters around B particles.

find that the change in the distribution of the frequency of the clusters might be the much more important mechanism for lowering the enthalpy than the lowering of the energy of an individual cluster.

Before we address this question further we briefly comment on a different observation. From Fig. 12 we recognize, that the observation we made in Fig. 9(a), namely that the curve for the AA coordination number $z=11$ is independent of the cooling rate, does not imply that the composition of the clusters containing 11 A atoms is independent of γ . Rather we see that the curves for cluster types $A_{14,3}$ and $A_{12,1}$, both of them having 11 A particles, show a quite strong dependence on γ . However, this dependence is such that they essentially cancel each other, i.e., that the γ depen-

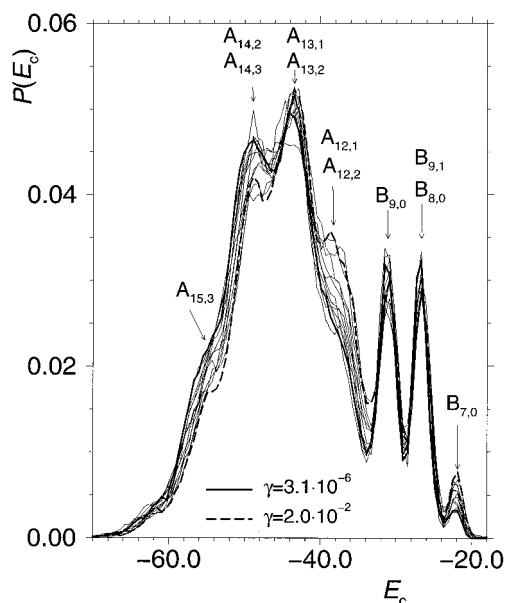


FIG. 13. Probability that a cluster has an energy E_c for all cooling rates investigated. The solid and dashed bold lines correspond to the smallest and largest cooling rate, respectively. The labels of the peaks identify the type of clusters that give rise to the corresponding peak.

dence of the abundance of the clusters containing 11 A particles is almost zero.

In order to understand the relative importance of the two above mentioned mechanisms to lower the enthalpy for the system with decreasing cooling rate, i.e., the lowering of the energy of each individual cluster and the changing of the distribution function $P_{\alpha_{\mu,\nu}}$, it is useful to look at $P(E_c)$, the probability that a cluster has an energy E_c . In Fig. 13 we show this probability for all cooling rates investigated. We see that this distribution shows various peaks, each of which can be related to certain types of clusters (see the labels). It should be noted that the *position* of a peak is related to the average energy E_c of the corresponding cluster and that the *height* of a peak is related to the frequency with which it occurs. We recognize from the figure that the main difference between the distribution for the slowest cooling rate (solid bold curve) and the fastest cooling rate (dashed bold curve) is that the height of the various peaks is significantly different. The frequency of cluster types, i.e. the value of $P(E_c)$, with high energies is decreasing and the one of cluster types with low energies is increasing with decreasing γ . The location of the peaks, however, shows only a very small change in the direction of lower energies, in accordance with point (1) in our discussion of Fig. 11. Thus we come to the conclusion that the *main* reason for the observed decrease of the enthalpy of the system with decreasing cooling rate is not that the energy of the individual clusters is decreasing, but that the distribution of the frequency with which these clusters occur shows a relatively strong dependence on the cooling rate.

From Fig. 13 we also easily recognize that icosahedral-like clusters, i.e., clusters in which a central particle is sur-

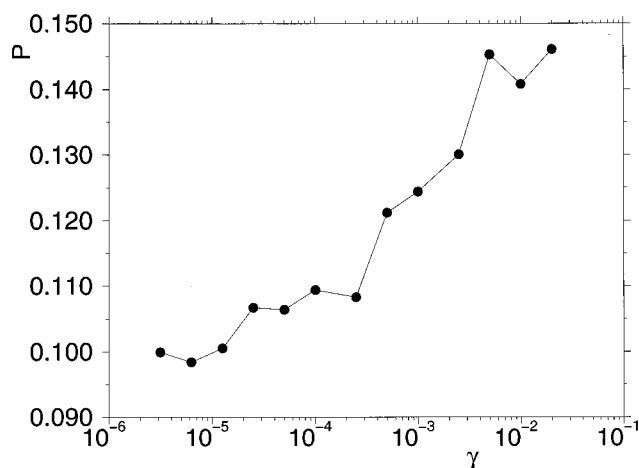


FIG. 14. Probability that a particle is in the center of an icosahedral-like structure versus the cooling rate.

rounded by 12 other particles, are not the most frequent local structures since clusters in which the A particle is surrounded by 13 or 14 particles are more common. As mentioned earlier, this observation is not in contradiction with the results of Jónsson and Andersen,²⁵ where it was shown that the frequency of certain *building blocks* for icosahedra is increasing with decreasing temperature. Jónsson and Andersen also reported that the probability that a given cluster is icosahedral-like is about 9% which is reasonably close to our value of 12% for intermediate cooling rates. Figure 13 also shows that the frequency of icosahedral-like clusters is *decreasing* with decreasing cooling rate from which it follows that this frequency decreases with decreasing temperature. To demonstrate this more clearly we show in Fig. 14 the probability that a particle is surrounded by 12 other particles, i.e. that it is the center of an icosahedral-like structure. From this figure we clearly recognize that this probability is decreasing with decreasing cooling rate. Thus we conclude from our results and the ones of Jónsson and Andersen that, although the frequency of typical building blocks for icosahedral-like structures increases with decreasing temperature, the icosahedral-like structures themselves *do not* become more frequent with decreasing temperature.

Similar to our definition of the energy of a cluster it is also possible to introduce the density of a cluster. Therefore it is possible to investigate how the distribution of the density of the clusters depend on the cooling rate and we found that, as is the case for the enthalpy, it is the cooling rate dependence of the distribution of the clusters, rather than the density of the clusters themselves, that is the main reason for the observed cooling rate dependence of the total density of the system.¹³

To close the subsection containing the results of our analysis of the cooling rate dependence of the glass at zero temperature, we present the results of our investigation about the spectrum of the glass. In order to gain some insight into the nature of the so-called boson peak (see, e.g., Ref. 27), the low-temperature spectrum of glass has in recent years been the focus of several investigations in which it was attempted

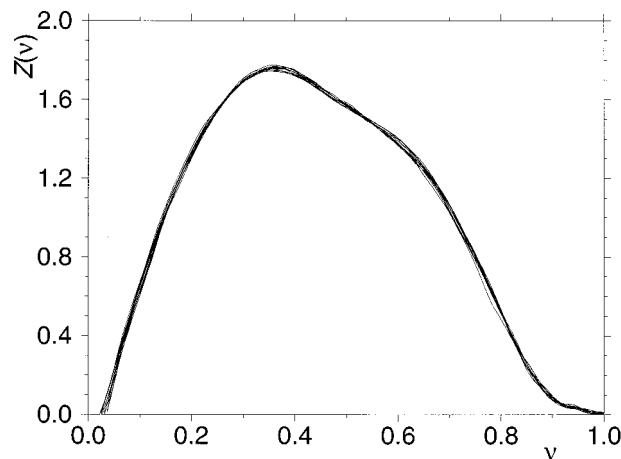


FIG. 15. $Z(\nu)$, the spectrum of the system at $T=0$ for all cooling rates investigated.

to address this question by means of computer simulations.^{28–31} Laird and Schober showed that in a glass in which the particles interact with a soft sphere potential there exist localized low-frequency modes which might be related to the boson peak,²⁸ a result which was also found for a model glass for selenium,³⁰ and recently Bembenek and Laird have also investigated the connection between the shape of the spectrum and the glass transition.³¹ In view of this work it is therefore interesting to see how the spectrum is affected when the cooling rate with which the glass was produced is changed.

We determined the spectrum of a given relaxed configuration at $T=0$ by computing the eigenvalues of the dynamical matrix, i.e., of $\partial^2 V(\{\mathbf{r}_i\})/\partial r_{j,\alpha}\partial r_{k,\beta}$, where j and k are particle indices and α and β are the Cartesian components x, y, z . From each configuration we thus obtained $3N$ eigenvalues λ , where N is the total number of particles, i.e., 1000. From these eigenvalues, all of which are non-negative, since the configuration is locally stable, we computed the frequencies $\nu = \sqrt{\lambda/m}/2\pi$. In Fig. 15 we show the so obtained spectrum $Z(\nu)$ for all cooling rates investigated. Not included in this figure are the three trivial eigenvalues of zero which correspond to a mere translation of the system. A comparison of this figure with the spectra shown in Ref. 30 for Se shows that the latter spectra are more structured, i.e. show more peaks than the one for the Lennard-Jones mixture. This difference is probably due to the fact that the potential of the models investigated by the authors of Ref. 30 tries to mimic directional bonds, whereas the Lennard-Jones model investigated here is more similar to a hard sphere model, with the corresponding packing structure, and we find that our spectrum is indeed qualitatively similar to the one of real metallic glasses.³² This argument is given further support by our observation that also the network forming glass SiO_2 shows a spectrum which is much more structured than the one for the Lennard-Jones system presented here.¹⁴

We recognize from Fig. 15 that the spectrum shows only a weak dependence on the cooling rate. That there actually is, however, such a dependence is shown in Fig. 16(a), where

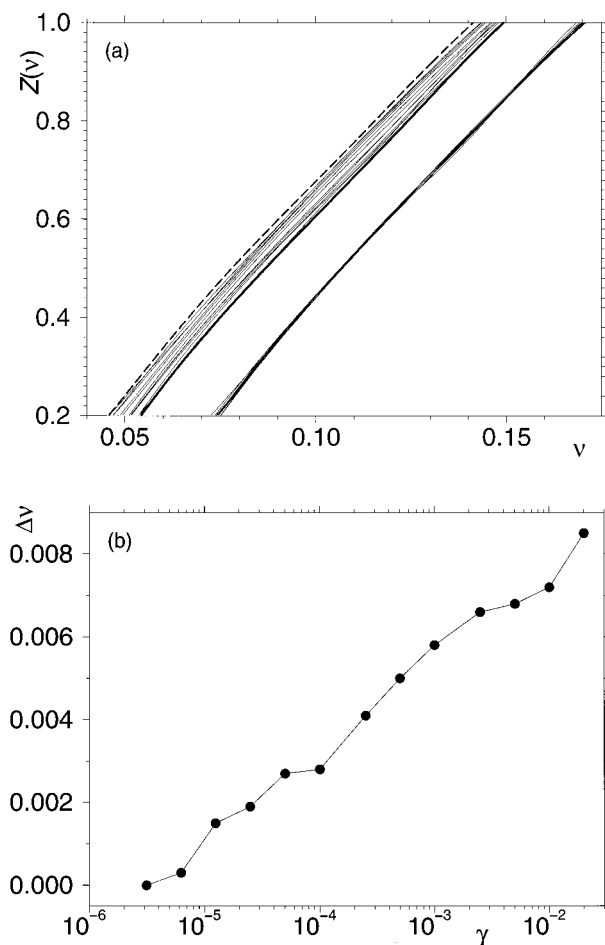


FIG. 16. (a) Low frequency part of the spectrum $Z(\nu)$ for all cooling rates investigated (left set of curves). The solid and dashed bold lines correspond to the smallest and largest cooling rate, respectively. The right set of curves are the same $Z(\nu)$ but now shifted by $\Delta\nu(\gamma)+0.02$ in order to collapse them onto a master curve (see the text for details). (b) The shift $\Delta\nu(\gamma)$ as a function of the cooling rate.

we show an enlargement of the low frequency part of the spectra. We clearly see that with decreasing cooling rate the spectrum moves to higher frequencies. A similar behavior is observed for the high frequency wing of the spectrum. Thus we come to the conclusion that with decreasing cooling rate the average local environment of the particles transforms in such a way that the local potential of the particles becomes stiffer. Such an effect is not implausible since we have seen that the density of the system increases with decreasing cooling rate and that therefore the particles are closer packed.

In order to estimate how large of an effect this shifting of the spectrum to higher frequencies is we proceeded as follows. From Fig. 16(a) we recognize that on the low frequency wing of the spectrum the main effect of the cooling rate seems to be that the spectrum is shifted to the right, i.e., without a change of the form of the curves. We therefore made use of this observation and attempted to shift the curves that have a value of γ larger than 3.1×10^{-6} , the smallest cooling rate, *horizontally*, i.e., in frequency, by an amount $\Delta\nu(\gamma)$ such that they collapsed as well as possible

with the curve for $\gamma=3.1 \times 10^{-6}$ in the range where the values of $Z(\nu)$ is between 0.2 and 1.0. The quality of the collapse between two curves was determined with the Spearman rank order correlation coefficient¹² and the shift $\Delta\nu(\gamma)$ was determined by maximizing this coefficient. In Fig. 16(a) we show the so obtained master curve (right set of curves). (In order to make the figure clearer we shifted this master curve by 0.02 to higher frequencies.) We thus recognize that it is indeed possible to collapse the curves for the different cooling rates onto one master curve, which shows that our procedure to estimate the frequency shift of the spectra as a function of the cooling rate is reasonable. In Fig. 16(b) we show the amount of shifting $\Delta\nu(\gamma)$ as a function of γ . We see that there is a clear trend that $\Delta\nu$ decreases with decreasing γ , i.e., that the low frequency part of the spectra moves to higher frequencies. It is interesting to note that the curve $\Delta\nu(\gamma)$ is approximated quite well by a straight line, i.e., that there is no indication that the spectrum converges towards an asymptotic distribution with decreasing γ . This means that with respect to this quantity we are not yet seeing the asymptotic behavior expected for very small values of γ , thus giving us evidence that there might be, at even smaller values of γ , a crossover from the γ dependence of $\Delta\nu$ we are observing here, to a different one. Note that this possibility is also in accordance with our finding in the context of the enthalpy of the system at $T=0$, where we also had some evidence that there might be a crossover at even smaller cooling rates than the ones considered here.

Although the effect observed here is relatively small, and therefore will probably not affect the conclusions drawn in the work of Refs. 28,30,31, we mention that a similar investigation for the strong glass former SiO_2 has shown that there are systems where the spectrum is strongly affected by the cooling rate.¹⁴ Thus such effects should probably be taken into account in the future.

Apart from this cooling rate dependence of the spectrum we recognize from Fig. 15 that $Z(\nu)$ also has a system size dependence, since the spectrum shows a gap at low frequencies. One knows that acoustic phonons with long wavelength do exist in a glass, as they exist in a crystalline solid. Phase space arguments imply that $Z(\nu) \propto \nu^2$ for $\nu \rightarrow 0$. This is not found in the simulation, since the finite linear dimension L of the box implies that the largest phonon wavelength is given by L . Hence the corresponding frequency is the lowest frequency occurring in the spectrum. Thus this finite size effect should be taken into account if one simulates very small systems.

IV. SUMMARY AND CONCLUSIONS

We have performed a molecular dynamics computer simulation of a binary Lennard-Jones system in order to investigate the dependence of the properties of a glass on its production history. In order to do this we cooled the system, with a cooling rate γ , from its high temperature liquid phase to a glass at zero temperature, and investigated how the glass transition as well as the so produced glass depend on this cooling rate.

In qualitative accordance with experiments^{1,2} we find that the glass transition becomes sharper with decreasing cooling rate, which is also in accordance with simple arguments put forward by Angell *et al.*¹⁶ In particular we see, that in the glass transformation range, the specific heat as well as the thermal expansion coefficient show a more rapid change the smaller the cooling rate is. Also the glass transition temperature T_g shows a cooling rate dependence and we demonstrate that this dependence can be understood by assuming that the temperature dependence of the relaxation times of the system is given by either a Vogel–Fulcher law or a power-law.

Our analysis of the glass shows that its density, its enthalpy as well as its structural properties, such as the radial distribution function, the coordination numbers and bond–bond angles, show a relatively small, but nevertheless noticeable (on the order of a few percent) dependence on the cooling rate with which the glass was produced. By investigating the cooling rate dependence of nearest neighbor clusters we give evidence that the dependence of quantities like the enthalpy or the density is mainly caused by the cooling rate dependence of the distribution of the frequency with which the various types of clusters occur.

In addition we show that in the glass icosahedral-like structures are not the most frequent local structures and that their frequency is even decreasing with decreasing cooling rate. This makes it unlikely that such structures are very important for the glass transition itself.

Finally we have also investigated how the spectrum $Z(\nu)$ of the glass depends on the cooling rate. We find that $Z(\nu)$ shows only a weak dependence on γ and that the main effect seems to be that the whole spectrum is shifted towards higher frequencies, a behavior which is quite plausible. It is interesting to note that the amount $\Delta\nu(\gamma)$ by which the spectrum is shifted, does not show any tendency to saturate within the range of cooling rates that we are able to access. Therefore it seems that the range of cooling rates falls at least into three regimes. The first one includes the very fast cooling rates. In this regime the cooling process is essentially a steepest descent procedure and the dependence of the properties of the glass on the cooling rate is relatively weak. In the second regime some quantities, such as the glass transition temperature or the density, show a *relatively* strong dependence on the cooling rate, but this dependence seems to become weaker with decreasing cooling rate and thus an extrapolation to experimental values of the cooling rate seems to be feasible. However, there seem to be quantities, such as the shift $\Delta\nu(\gamma)$ of the spectrum or, to a lesser extent, the enthalpy of the system, which show in this second regime a cooling rate dependence which is not physically reasonable for arbitrarily small values of γ . Therefore we conclude that there must be a third regime of cooling rates in which *all* quantities actually show a cooling rate dependence which is the asymptotic one.

To conclude we can say that this work has shown that also in computer simulations the phenomenon of the glass transition, the macroscopic as well as the microscopic properties of the glass show a clear dependence on the cooling

rate and that some of these dependencies, such as the one of H and ρ can be understood also from a microscopic point of view. For the model investigated here these effects are relatively small but we know that they might be substantial in other types of systems.¹⁴ Therefore it is advisable that in future simulations which investigate the glass transition, this aspect is not left out since, e.g., the outcome of investigations in which it is tested whether a specific model is able to reproduce experimental properties of glass, might be severely affected by the history on how the glass was produced on the computer.

ACKNOWLEDGMENTS

We thank C. A. Angell for valuable discussions. K.V. thanks Schott-Glaswerke, Mainz and the DFG, through SFB 262, for financial support. Part of this work was done on the computer facilities of the Regionales Rechenzentrum Kaiserslautern.

- ¹R. Brüning and K. Samwer, *Phys. Rev. B* **46**, 11318 (1992).
- ²See, e.g., H. N. Ritland, *J. Am. Ceram. Soc.* **37**, 370 (1954); C. Y. Yang, D. E. Sayers, and M. A. Paesler, *Phys. Rev. B* **36**, 8122 (1987); C. T. Limbach and U. Gonser, *J. Non-Cryst. Solids* **106**, 399 (1988); G. P. Johari, A. Hallbrucker, and E. Mayer, *J. Phys. Chem.* **93**, 2648 (1989); R. Brüning and M. Sutton, *Phys. Rev. B* **49**, 3124 (1994).
- ³J. R. Fox and H. C. Andersen, *J. Phys. Chem.* **88**, 4019 (1984).
- ⁴J. Baschnagel, K. Binder, and H.-P. Wittmann, *J. Phys.* **5**, 1597 (1993).
- ⁵S. K. Lai and M. S. Lin, *J. Non-Cryst. Solids* **117/118**, 907 (1990).
- ⁶H. Miyagawa and Y. Hiwatari, *Phys. Rev. A* **40**, 6007 (1989).
- ⁷R. Speedy, *Mol. Phys.* **83**, 591 (1994).
- ⁸W. Kob, *Annual Reviews of Computational Physics*, edited by D. Stauffer (World Scientific, Singapore, 1995), Vol. III, p. 1.
- ⁹W. Kob and H. C. Andersen, *Phys. Rev. Lett.* **73**, 1376 (1994); *Phys. Rev. E* **51**, 4626 (1995); **52**, 4134 (1995).
- ¹⁰T. A. Weber and F. H. Stillinger, *Phys. Rev. B* **31**, 1954 (1985).
- ¹¹H. C. Andersen, *J. Chem. Phys.* **72**, 2384 (1980); see also Ref. 3.
- ¹²W. H. Press, S. A. Teukolsky, W. T. Vetterling, and B. P. Flannery, *Numerical Recipes* (Cambridge University Press, Cambridge, 1992).
- ¹³K. Vollmayr, Ph.D. thesis, Universität Mainz, 1995.
- ¹⁴K. Vollmayr, W. Kob, and K. Binder (unpublished); K. Vollmayr and W. Kob, *Ber. Bunsenges. Phys. Chem.* (in press).
- ¹⁵C. H. Reinsch, *Num. Math.* **10**, 177 (1967); **16**, 451 (1971).
- ¹⁶C. A. Angell, J. H. R. Clarke, and L. V. Woodcock, *Adv. Chem. Phys.* **48**, 397 (1981); see also C. A. Angell and L. M. Torell, *J. Chem. Phys.* **78**, 937 (1983).
- ¹⁷A. Q. Tool and C. G. Eichlin, *J. Opt. Soc. Am.* **14**, 276 (1931).
- ¹⁸See, e.g., W. Götze and L. Sjögren, *Rep. Prog. Phys.* **55**, 241 (1992).
- ¹⁹W. Kob and R. Schilling, *J. Phys. A* **23**, 4673 (1990), and references therein.
- ²⁰G. S. Grest, C. M. Soukoulis, and K. Levin, *Phys. Rev. Lett.* **56**, 1148 (1986); G. S. Grest, C. M. Soukoulis, K. Levin, and R. E. Randleman, in *Heidelberg Colloquium on Glassy Dynamics*, Lecture Notes in Physics, Vol. 275, edited by J.L. van Hemmen and I. Morgenstern (Springer, Berlin, 1987); D. A. Huse and D. S. Fisher, *Phys. Rev. Lett.* **57**, 2203 (1986).
- ²¹S. Cornell, K. Kaski, and R. B. Stinchcombe, *J. Phys. A* **24**, L865 (1991); J. Jäckle, R. B. Stinchcombe, and S. Cornell, *J. Stat. Phys.* **62**, 425 (1991); S. Shinomoto and Y. Kabashima, *J. Phys. A* **24**, L141 (1991); P. Sibani, J. M. Pedersen, K. H. Hoffmann, and P. Salamon, *Phys. Rev. A* **42**, 7080 (1990).
- ²²J.-P. Hansen and I. R. McDonald, *Theory of Simple Liquids* (Academic, London, 1986).
- ²³K. Vollmayr, W. Kob, and K. Binder, in *Computer Simulation Studies in Condensed Matter Physics*, edited by D. P. Landau, K. K. Mon, and H. B. Schüttler (Springer, Berlin, 1995), Vol. III, p. 117.
- ²⁴For a discussion on the nature of the nearest neighbor shells of simple atomic liquids see J. Sietsma and B. J. Thiesse, *Phys. Rev. B* **52**, 3248 (1995); S. Cozzini and R. Ronchetti (unpublished).
- ²⁵H. Jónsson and H. C. Andersen, *Phys. Rev. Lett.* **60**, 2295 (1988).

- ²⁶K. Vollmayr, W. Kob, and K. Binder, *Europhys. Lett.* **32**, 715 (1995).
- ²⁷See, e.g., *Physica A* **201** (1993).
- ²⁸B. B. Laird and H. R. Schober, *Phys. Rev. Lett.* **66**, 636 (1991); H. R. Schober and B. B. Laird, *Phys. Rev. B* **44**, 6746 (1991).
- ²⁹B. M. Forrest, E. Leontidis, and U. W. Suter, *J. Chem. Phys.* **104**, 2401 (1996); V. Mazzacurati, G. Ruocco, and M. Sampoli (unpublished).
- ³⁰H. R. Schober and C. Oligschleger, *Nukleonika* **39**, 185 (1994); C. Oligschleger and H. R. Schober, *Physica A* **201**, 391 (1993); C. Oligschleger, Ph.D. thesis, Jülich, 1994; H. R. Schober, C. Oligschleger, and B. B. Laird, *Non-Cryst. Solids* **156-158**, 965 (1993); H. R. Schober and C. Oligschleger, *Phys. Rev. B* **52**, 11469 (1996); M. Garcia-Hernandez *et al.*, *Phys. Rev. B* **48**, 149 (1993); N. G. Almaraz, E. Enciso, and F. J. Bermejo, *J. Chem. Phys.* **99**, 6876 (1993).
- ³¹S. D. Bembek and B. B. Laird, *Phys. Rev. Lett.* **74**, 936 (1995); *J. Chem. Phys.* **104**, 5199 (1996).
- ³²See, e.g., J.-B. Suck and H. Rudin, in *Glassy Metals*, edited by H. Beck and H.-J. Güntherodt (Springer; Berlin, 1983) Vol. II, p. 217; J.-B. Suck, in *Rapidly Quenched Metals*, edited by S. Steeb and H. Warlimont (Elsevier, Amsterdam, 1985), p. 471; J.-B. Suck, H. Rudin, H.-J. Güntherodt, and H. Beck, *Non-Cryst. Solids* **61&62**, 295 (1984); J.-B. Suck (unpublished).